Fluid Phase Equilibria 294 (2010) 234–240

Contents lists available at ScienceDirect

Fluid Phase Equilibria

journal homepage: www.elsevier.com/locate/fluid

Solubility of non-aromatic ionic liquids in water and correlation using a QSPR approach

Mara G. Freire [a], Catarina M.S.S. Neves [a], Sónia P.M. Ventura [a], Maria J. Pratas [a], Isabel M. Marrucho [a], João Oliveira [b], João A.P. Coutinho [a], Ana M. Fernandes [c,*]

[a] CICECO, Departamento de Química, Universidade de Aveiro, Campus Universitario de Santiago, 3810-193 Aveiro, Portugal
[b] CESAM, Departamento de Química, Universidade de Aveiro, 3810-193 Aveiro, Portugal
[c] QOPNA, Departamento de Química, Universidade de Aveiro, 3810-193 Aveiro, Portugal

ARTICLE INFO

Article history:
Received 31 October 2009
Received in revised form
23 December 2009
Accepted 29 December 2009
Available online 11 January 2010

Keywords:
Ionic liquids
Water
Mutual solubilities
ESI-MS
Thermodynamic functions
QSPR

ABSTRACT

The solubility of ionic liquids (ILs) in water is of significant relevance for both process design and evaluation of their environmental impact. In this work, the solubilities of the non-aromatic piperidinium- and pyrrolidinium-based ILs in water, combined with the anion bis(trifluoromethylsulfonyl)imide, were determined in the temperature range from (288.15 to 318.15) K. Electrospray ionization mass spectrometry (ESI-MS) was used as the analytical method after a proper validation of the experimental results obtained. The effect of the ILs structural combinations, such as cation family and alkyl side chain length, in their solubility in water, is analyzed and discussed. From the ILs solubility dependence on temperature, the standard molar thermodynamic functions of solution, namely Gibbs energy, enthalpy and entropy at infinite dilution, were determined. The results indicate that the ILs dissolution in water is an endothermic process and entropically driven. To predict the mutual solubilities between ILs and water, a quantitative structure–property relationship (QSPR) model is also proposed. It is shown that it can provide a good description of the mutual solubilities at 303.15 K with deviations smaller than 10%.

1. Introduction

Ionic liquids (ILs) are low-melting salts that result from the combination of large organic cations with various alkyl substituents and either inorganic or organic anions. Interest in exploring the properties and applications of ILs in a variety of fields, ranging from fundamental science to technology, has been intensified due to their unusual performances and their potential as "green" replacements for the conventional volatile, flammable and toxic organic solvents, as well as the possibility of recycling them, that could lead to a large improvement on processes safety and efficiency [1–4].

Although ILs are generally referred to as "green" solvents, studies on their toxicity and biodegrability are vital issues. While ILs cannot vaporize leading to air pollution (due to their negligible vapor pressures), all of them present some miscibility with water – even in the limit of infinite dilution – that may be the cause of environmental aquatic concerns. The ILs ecotoxicity can be directly linked to their hydrophilic/lipophilic nature [5–11]. Even though large immiscibility gaps exist between hydrophobic ILs and water, these ILs are indeed more toxic than hydrophilic ones, because of their higher aptitude to accumulate in biological membranes. Therefore, the knowledge of the ILs solubility in water can provide relevant information on the toxicity and bioaccumulation impact of a specific IL in the ecosystem [5–11]. Note, however, that some exceptions to this general relationship exist depending on the aquatic organisms, exposure conditions and evaluation methods, among others. Indeed, recent results from our group show that aromatic ILs are substantially more toxic than non-aromatic ones [12].

Much attention has been dedicated to hydrophilic ILs, yet hydrophobic ILs are gaining considerable relevance in analytical chemistry and separation technology. IL-water two-phase systems have been currently applied in the extraction of low molecular weight neutral compounds, biopolymers and ions, and several reviews on extraction applications using hydrophobic ILs are available [13–17]. In addition, hydrophobic ILs are being explored for potentiometric and voltammetric sensors, and in two-phase organic synthesis [18]. In all approaches the knowledge of the cross contamination between the IL and the second liquid phase is a crucial factor. In spite of the importance of ILs and water liquid–liquid equilibria, only scattered data have been reported [9–11,19–31]. Moreover, systematic studies for selected ILs, in a wide temperature range, are scarce [9–11]. The solubility in water of the heterocyclic imidazolium- and pyridinium-based ILs has

* Corresponding author. Tel.: +351 234 370200; fax: +351 234 370084.
E-mail address: afernandes@ua.pt (A.M. Fernandes).

0378-3812/$ – see front matter © 2010 Elsevier B.V. All rights reserved.
doi:10.1016/j.fluid.2009.12.035

been determined using UV–vis spectroscopy, since both of these cations present characteristic absorption peaks in the ultraviolet region of the electromagnetic spectrum [9–11]. Nevertheless, for ILs with pyrrolidinium- and piperidinium-based cations the maximum absorption in the UV region occurs at wavelengths lower than 190 nm, due to the absence of π molecular orbitals, requiring a distinct quantification method. Electrospray ionization mass spectrometry (ESI-MS) [32–33] is a powerful technique for the analysis of positive and negative ions present in solution, and is here proposed as an alternative quantification method for the determination of ILs solubility in water. The production of gas phase ions from solutions in the electrospray ionization process, involves two main steps: (a) production of charged droplets at a capillary tip and (b) shrinkage of charged droplets due to solvent evaporation and repeated droplet fission leading to gas phase ions (and that can be analyzed in the mass spectrometer). A high voltage (typically 2–3 kV) is applied to a metallic capillary (1 mm o.d.) through which the solution is flowing at a flow rate of 10 mL min^{-1}. The strength of the electric field at the capillary tip is typically around 10^6–10^7 V m^{-1}. In the positive mode, anions migrate in the direction of the capillary, whereas cations migrate in the direction of the counterelectrode, which is located 2–3 cm from the capillary tip. At sufficiently high electric field strengths, a dynamic cone of liquid, a Taylor cone, will form at the tip of the capillary. If the applied field is sufficiently high, the tip becomes unstable and a fine jet emerges from the cone tip. The repulsion between charges causes the jet to break up into smaller droplets. As the solvent evaporates from the droplets with the assistance of warm nitrogen gas, the size of the droplets decreases until the electrostatic repulsion between the ions becomes equal to the surface tension, and droplet fission occurs. Successive fissions will ultimately lead to the formation of gas phase ions that can be analyzed within the mass spectrometer. A unique feature of this technique is the direct transfer of ions present in solution to the gas phase. Therefore, in this work, the ESI-MS approach was rigorously validated with previous results obtained for the solubility of 1-butyl-3-methylimidazolium hexafluorophosphate in water [9], and subsequently applied in the determination of original solubility data for 1-methyl-1-propylpyrrolidinium bis(trifluoromethylsulfonyl)imide, 1-butyl-1-methylpyrrolidinium bis(trifluoromethylsulfonyl)imide, and 1-methyl-1-propylpiperidinium bis(trifluoromethylsulfonyl)imide, in the temperature range from (288.15 to 318.15) K and at atmospheric pressure. From the results obtained, the impact of the ILs structure, such as the cation family and the alkyl side chain length, were evaluated. Furthermore, from the solubility data dependence on temperature, thermodynamic molar solution properties were determined and discussed.

Quantitative Structure–Activity Relationships (QSAR) and Quantitative Structure–Property Relationships (QSPR) are methods for direct prediction of activities or properties of compounds based on their molecular structure. These models correlate experimental data with specific parameters, named molecular descriptors, derived from the compound's 3D structure [34–35]. QSAR/QSPR models are especially apt for the development of original drugs, conception of novel molecules, molecular modelling and resolution of new problems related with chemical engineering. Yet, QSAR/QSPR methods require a large experimental database aiming at obtaining accurate correlations prior to their effective use. These models can be further used as predictive instruments for the estimation of physical–chemical properties, identifying the most favourable compounds for a specific purpose, and thus orienting the synthesis and reducing the number of compounds to be synthesized. This fact is of main interest when dealing with the extremely large number of possible combinations between cations and anions in ILs and their tailoring capacity. Indeed, QSPR studies have already been used in correlations and predictions of various properties of ILs such as melting points [36], conductivities and viscosities [37]. A QSPR method was here applied for the first time to describe the mutual solubilities between water and ILs at 303.15 K, after compiling a sufficiently large database regarding water and ILs liquid–liquid equilibria [9–11,20].

2. Solubility of non-aromatic ionic liquids in water

2.1. Materials and experimental procedure

The experimental aqueous solubility was performed for the ILs 1-butyl-3-methylimidazolium hexafluorophosphate, [C_4mim][PF_6], 1-methyl-1-propylpyrrolidinium bis(trifluoromethylsulfonyl)imide, [C_3mpyr][Tf_2N], 1-butyl-1-methylpyrrolidinium bis(trifluoromethylsulfonyl)imide, [C_4mpyr][Tf_2N], and 1-methyl-1-propylpiperidinium bis(trifluoromethylsulfonyl)imide, [C_3mpip][Tf_2N]. The ILs used as internal standards were 1-butyl-3-methylimidazolium tetrafluoroborate, [C_4mim][BF_4], and 1-methyl-3-propylimidazolium bis(trifluoromethylsulfonyl)imide, [C_3mim][Tf_2N]. All ILs were acquired at Iolitec within a halides content <100 ppm. To reduce the water and volatile compounds content to negligible values, ILs individual samples were dried under constant stirring, under vacuum at 0.1 Pa and temperature at 353 K, for a minimum of 48 h. After this procedure, the purity of each IL was additionally checked by ^{1}H, ^{13}C and ^{19}F NMR spectra and found to be >99 wt%. The water used was ultrapure water, double distilled, passed by a reverse osmosis system and treated with a Milli-Q plus 185 water purification apparatus. The water used presents a resistivity of 18.2 MΩ cm, a TOC smaller to 5 μg dm^{-3} and is free of particles >0.22 μm. The methanol used was from Lab-Scan and >99.9 wt% pure.

Solubilities of the ILs in water were carried out at temperatures from (288.15 to 318.15) K (5 K intervals) and at atmospheric pressure. The IL and water phases (10 cm^3 of each) were initially vigorously agitated and allowed to reach the mutual saturation by the separation of both phases, in sealed glass vials, for at least 48 h. The temperature was maintained by keeping the glass vials inserted in an aluminium block specially designed for the purpose. The aluminium block was placed in an isolated air bath capable of maintaining the temperature within ±0.01 K. The temperature control was achieved using a PID temperature controller driven by a calibrated Pt100 (class 1/10) temperature sensor inserted in the aluminium block. In order to reach the temperatures below room temperature a Julabo circulator, model F25-HD, was coupled to the overall oven system allowing the passage of a thermostatized fluid flux around the aluminium block. The water-rich phases were sampled using glass syringes maintained dry and at the same temperature of the measurements. Samples of ≈1.0 g were taken and diluted by a factor of 1:20 (v/v) or 1:50 (v/v) in a 1:1 (v/v) mixture of ultrapure water and methanol containing a previously and fixed amount of internal standard ([C_4mim][BF_4] for [C_4mim][PF_6] quantification and [C_3mim][Tf_2N] for [C_3mpyr][Tf_2N], [C_4mpyr][Tf_2N] and [C_3mpip][Tf_2N] quantification). The internal standards were also used in the calibration curves determination and at constant concentration. For the calibration curve of [C_4mim][PF_6], a fixed amount (201.6 mg dm^{-3}) of the internal standard [C_4mim][BF_4] was added to each of the six standard solutions of concentrations 50.0, 100.0, 213.6, 320.4, 405.8 and 500.0 mg dm^{-3} in the solvent mixture CH_3OH:H_2O (1:1, v/v). For the calibration curves of [C_3mpip][Tf_2N], [C_3mpyr][Tf_2N] and [C_4mpyr][Tf_2N] a fixed amount (≈250 mg dm^{-3}) of the internal standard [C_3mim][Tf_2N] was added to each of the seven standard solutions with concentrations ranging from 50.0 to 800.0 mg dm^{-3} in the solvent mixture CH_3OH:H_2O (1:1, v/v).

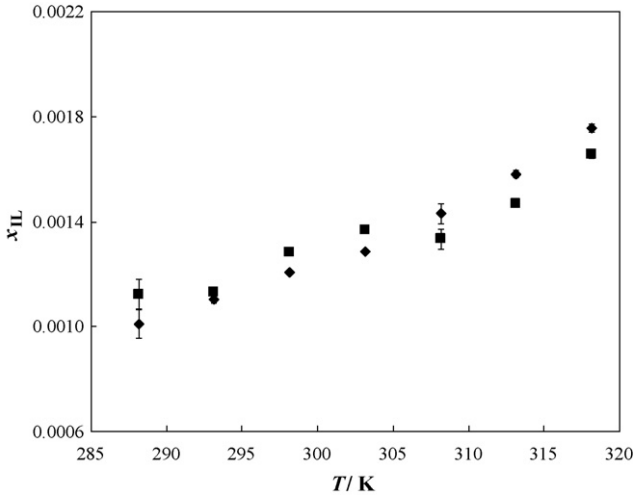

Fig. 1. Mole fraction solubility of $[C_4mim][PF_6]$ in water as a function of temperature determined by (♦) UV–vis spectroscopy [9] and (■) ESI-MS (this work).

The ILs quantification was determined using a Micromass Quattro LC triple quadrupole mass spectrometer using the calibration curves previously established. The operating conditions of the mass spectrometer were the following: source and desolvation temperatures of 353 K and 423 K, respectively; capillary voltage of 3000 V (or 2600 V for the negative ion mode); and cone voltage of 25 V. N_2 was used as the nebulization gas and the diluted samples (1:1000, v/v) were introduced at a 10 mL min^{-1} flow rate using the methanol–water (1:1, v/v) mixture as the eluent solvent. For the measurement of peak abundances, an average of 100 scans for each mass spectrum was used. Triplicate independent sampling measurements were performed for both standards and samples.

2.2. Results and discussion

The solubility of $[C_4mim][PF_6]$ in water, using $[C_4mim][BF_4]$ as internal standard, was determined and compared with the results obtained previously using UV–vis spectroscopy [9] in order to ascertain the reliability of the ESI-MS as an alternative quantification method. The ESI-MS of the ILs solutions in the negative ion mode showed peaks at m/z 145 and 87, corresponding to ions $[PF_6]^-$ (analyte) and $[BF_4]^-$ (internal standard), respectively. The relative abundances of ions m/z 145 and 87 were measured, in triplicate, and the plot of the abundances ratio as function of the respective concentrations ratio (calibration curve) is provided in Supporting Information. The linear dependence, in the concentration range used, is expressed by the fine correlation coefficient of 0.9979.

The water solubility of $[C_4mim][PF_6]$ at the temperatures from (288.15 to 318.15) K, was experimentally determined using $[C_4mim][BF_4]$ as internal standard and ionic abundances measured in three independent aliquots for each temperature. The experimental solubility values thus obtained are presented in Fig. 1, together with the values reported before using the UV–vis spectroscopic technique [9]. The solubility values obtained by mass spectrometry are, with the exception of the value at 288.15 K, within 5% of the ones obtained by UV–vis spectroscopy [9] and no systematic errors were observed. The results obtained by both techniques are in close agreement and reveal the possibility of using an alternative method for the quantification of ILs in aqueous solutions.

The experimental procedure and data treatment described previously were further used for the determination of the solubilities of ILs that do not have a significant absorbance in the UV–vis region, due to lack of aromaticity or insaturation in their cations (pyrrolidinium and piperidinium). The internal standard chosen was $[C_3mim][Tf_2N]$ which shows a peak at m/z 125 in the ESI-MS derived from the cation. Note that cluster ions of internal standard and sample ILs, whenever formed, had a relative abundance smaller than 1%, which falls within the standard deviation of the internal standard and sample relative abundances [38]. Calibration curves (plot of the ratio of relative abundances of the cations corresponding to each IL to the internal standard, $[C_3mim]^+$ with m/z 125, as a function of the respective concentrations ratio) for the three ILs studied are presented in Supporting Information.

Table 1
Mole fraction solubility of ILs in water, x_{IL}, at different temperatures, and respective standard deviation (σ).

T (K)	$[C_4mim][PF_6]$ 10^3 ($x_{IL} \pm \sigma$)	$[C_3mpip][Tf_2N]$ 10^4 ($x_{IL} \pm \sigma$)	$[C_3mpyr][Tf_2N]$ 10^4 ($x_{IL} \pm \sigma$)	$[C_4mpyr][Tf_2N]$ 10^4 ($x_{IL} \pm \sigma$)
288.15	1.12 ± 0.06	3.42 ± 0.22	4.15 ± 0.03	2.14 ± 0.09
293.15	1.13 ± 0.01	3.59 ± 0.21	4.45 ± 0.08	2.32 ± 0.09
298.15	1.28 ± 0.01	3.68 ± 0.03	4.36 ± 0.04	2.38 ± 0.01
303.15	1.37 ± 0.01	3.86 ± 0.16	4.81 ± 0.20	2.31 ± 0.11
308.15	1.33 ± 0.04	4.18 ± 0.07	4.85 ± 0.03	2.52 ± 0.01
313.15	1.47 ± 0.01	4.51 ± 0.24	5.11 ± 0.05	2.67 ± 0.01
318.15	1.66 ± 0.02	4.63 ± 0.03	5.37 ± 0.03	2.94 ± 0.11

The mole fraction solubilities of the studied ILs in water are presented in Table 1 and Fig. 2. In Fig. 2 experimental data obtained previously [9,11] for 1-methyl-3-propylimidazolium bis(trifluoromethylsufonyl)imide, $[C_3mim][Tf_2N]$, and 3-methyl-1-propylpyridinium bis(trifluoromethylsulfonyl)imide, $[C_3mpy][Tf_2N]$, were also included for comparison purposes. In general, an increase in the solubility of ILs in water was observed with the temperature increase, meaning that these two-phase systems should present an upper critical solution temperature.

From Fig. 2, the results obtained indicate that the ILs solubility in water at a constant temperature follows the order: $[C_4mpyr]^+ < [C_3mpip]^+ < [C_3mpy]^+ < [C_3mpyr]^+ < [C_3mim]^+$. However, the trend observed before for the water solubility in the IL-rich phase [9] was the following: $[C_4mpyr]^+ < [C_3mpip]^+ < [C_3mpyr]^+ < [C_3mpy]^+ < [C_3mim]^+$. The differences in solubilities observed in both phases, indicate that the solubility of water in ILs largely depends on the IL availability of electrons for privileged interactions with water. Aromatic ILs present a higher solvation capability for water than aliphatic ones. On the opposite, the solubility of ILs in water seems to be primarily controlled by the cation size, and, to a lower extent, by their aromaticity. Indeed,

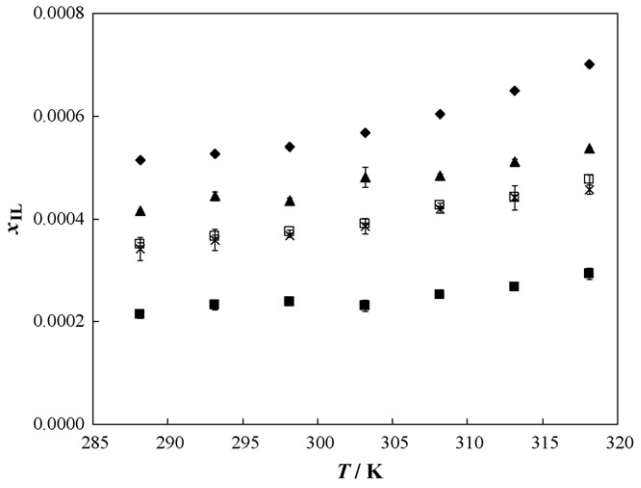

Fig. 2. Mole fraction solubility of ILs in water as a function of temperature: (♦) $[C_3mim][Tf_2N]$ [11]; (▲) $[C_3mpyr][Tf_2N]$; (□) $[C_3mpy][Tf_2N]$ [9]; (×) $[C_3mpip][Tf_2N]$; (■) $[C_4mpyr][Tf_2N]$.

the sequence obtained for the solubility of ILs in water follows the molar volumes trend of the respective ILs (at 288.15 K) [39]: $[C_4mpyr][Tf_2N]$ with 0.2998 $dm^3\,mol^{-1}$ < $[C_3mpip][Tf_2N]$ with 0.2981 $dm^3\,mol^{-1}$ < $[C_3mpy][Tf_2N]$ with 0.2861 $dm^3\,mol^{-1}$ < $[C_3mpyr][Tf_2N]$ with 0.2839 $dm^3\,mol^{-1}$ < $[C_3mim][Tf_2N]$ with 0.2729 $dm^3\,mol^{-1}$.

In order to determine the standard molar thermodynamic functions of solution, the experimental solubility of the studied ILs in water was correlated by Eq. (1):

$$\ln x_{IL} = A + \frac{B}{T/K} + C \ln\left(\frac{T}{K}\right) \quad (1)$$

where A, B and C are correlation parameters and x_{IL} is the mole fraction solubility of the IL at each specific temperature, T. The correlation parameters and respective standard deviations are presented in Table 2. The proposed correlation presents a maximum relative deviation from experimental mole fraction solubility data of 4% and it is useful for determining the ILs solubility in water at temperatures not experimentally available.

At the equilibrium state the chemical potentials of the IL at the aqueous-rich phase and at the IL-rich phase have to be equivalent, and the electroneutrality of both rich phases must be obeyed. In the current situation, the presence of ILs in the aqueous-rich phase can be considered at infinite dilution, and thus no main solute–solute interactions (electrostatic contribution) and/or ion-pairing subsist, allowing the determination of the standard molar thermodynamic functions of the ILs solution, such as standard molar enthalpy ($\Delta_{sol}H^0_m(T)$), molar Gibbs energy ($\Delta_{sol}G^0_m(T)$) and molar entropy ($\Delta_{sol}S^0_m(T)$) [9,11]. These associated thermodynamic properties are reported in Table 2, as well as the respective values for $[C_3mim][Tf_2N]$ and $[C_3mpy][Tf_2N]$ for a more global evaluation of the cation influence [9,11]. In addition, the standard deviations of such properties are provided in Table 2 and they were determined by the least squares regression analysis taking into account the standard deviations of the variables involved (B, C and T).

While the molar enthalpies of solution of water in ILs are temperature independent [9,11] the molar enthalpies of solution of ILs in water are significantly temperature dependent (in the studied temperature range). At 298.15 K, $\Delta_{sol}H^0_m$ indicates that the ILs dissolution is an endothermic process. Moreover, $\Delta_{sol}H^0_m$ shows to be almost independent of both the cation nature and the alkyl side chain length, corroborating thus the results obtained before where it was found that the IL anion nature is the main feature ruling such property [9]. On the other hand, the molar entropies of solution of $[C_3mpyr][Tf_2N]$ and $[C_4mpyr][Tf_2N]$ in water indicate a decrease of approximately – 5 $J\,K^{-1}\,mol^{-1}$ *per* methylene addition at the cation. Accordingly, the decrease of the ILs solubility in water is driven by the decrease in the molar entropy of solution. This decrease in the molar entropy of solution with the cation alkyl side chain length increase was already shown before for imidazolium-based ILs [9,11] and it is here proven that it is independent of the cation family, occurring also for pyrrolidinium-based ILs. Indeed, the molar entropies of solution are shown to be mainly dependent on the cation alkyl side chain length and on the anion nature [9,11], while the cation family seems to have no significant influence on such property. Indeed, the negative entropies of solution in combination with the positive Gibbs energies of solution are in agreement with the well known "hydrophobic effect" [40].

3. QSPR modelling of (ionic liquids + water) mutual solubilities

3.1. Experimental database

The mutual solubilities between water and 26 different ILs (both the IL solubility in the aqueous-rich phase and the water solubility in the IL-rich phase) were used in the present study. The solubility saturation values were obtained from this work and from literature [9–11,20]. The ILs studied were 1-methyl-3-propylimidazolium hexafluorophosphate, $[C_3mim][PF_6]$, 1-butyl-3-methylimidazolium hexafluorophosphate, $[C_4mim][PF_6]$, 1-hexyl-3-methylimidazolium hexafluorophosphate, $[C_6mim][PF_6]$, 1-methyl-3-octylimidazolium hexafluorophosphate, $[C_8mim][PF_6]$, 1-butyl-2,3-dimethylimidazolium hexafluorophosphate, $[C_4C_1mim][PF_6]$, 1,3-dimethylimidazolium bis(trifluoromethylsulfonyl)imide, $[C_1mim][Tf_2N]$, 1-ethyl-3-methylimidazolium bis(trifluoromethylsulfonyl) imide, $[C_2mim][Tf_2N]$, 1-methyl-3-propylimidazolium bis(trifluoromethylsulfonyl)imide, $[C_3mim][Tf_2N]$, 1-butyl-3-methylimidazolium bis(trifluoromethylsulfonyl)imide, $[C_4mim][Tf_2N]$, 1-methyl-3-pentylimidazolium bis(trifluoromethylsulfonyl)imide, $[C_5mim][Tf_2N]$, 1-hexyl-3-methylimidazolium bis(trifluoromethylsulfonyl)imide, $[C_6mim][Tf_2N]$, 1-heptyl-3-methylimidazolium bis(trifluoromethylsulfonyl)imide, $[C_7mim][Tf_2N]$, 1-methyl-3-octylimidazolium bis(trifluoromethylsulfonyl)imide, $[C_8mim][Tf_2N]$, 1-decyl-3-methylimidazolium bis(trifluoromethylsulfonyl) imide, $[C_{10}mim][Tf_2N]$, 1,3-diethylimidazolium bis(trifluoromethylsulfonyl)imide $[C_2C_2im][Tf_2N]$, 1-butyl-2,3-dimethylimidazolium bis(trifluoromethylsulfonyl)imide, $[C_4C_1mim][Tf_2N]$, 1-methyl-3-propylpyridinium bis(trifluoromethylsulfonyl)imide, $[C_3mpy][Tf_2N]$, 1-methyl-1-propylpyrrolidinium bis(trifluoromethylsulfonyl)imide, $[C_3mpyr][Tf_2N]$, 1-butyl-1-methylpyrrolidinium bis(trifluoromethylsulfonyl)imide $[C_4mpyr][Tf_2N]$, 1-methyl-1-propylpiperidinium bis(trifluoromethylsulfonyl)imide, $[C_3mpip][Tf_2N]$, 1-methyl-3-propylpyridinium hexafluorophosphate, $[C_3mpy][PF_6]$, 1-butyl-3-methylpyridinium bis(trifluoromethylsulfonyl)imide, $[C_4mpy][Tf_2N]$, 1-butyl-4-methylpyridinium bis(trifluoromethylsulfonyl)imide, $[4\text{-}C_4mpy][Tf_2N]$, butylpyridinium bis(trifluoromethylsulfonyl)imide, $[C_4py][Tf_2N]$, hexylpyridinium bis(trifluoromethylsulfonyl)imide, $[C_6py][Tf_2N]$ and octylpyridinium bis(trifluoromethylsulfonyl)imide, $[C_8py][Tf_2N]$.

3.2. Methodology

The structures and subsequent data files of both cation and anion for each IL were prepared using the ChemDraw Ultra 9.0-2004. The program Dragon®, version 5.3 – 2005, was used to calculate the descriptors. In order to correlate the mutual solubilities with the descriptors, the following equation based on LSER (Linear Solvation Energy Relationship) was applied:

$$\ln x = a + b \times \Delta_1 + c \times \Delta_2 + d \times \Delta_3 \quad (2)$$

where x is the mole fraction of water in IL or IL in water; a, b, c and d are correlation coefficients, Δ_1 is the cavity term, Δ_2 is a polarizability descriptor and Δ_3 is the descriptor related with hydrogen bonding.

Among the 1664 molecular descriptors calculated by Dragon® covering topological, molecular and 3D properties of the ions, the ones most similar to the Δ_i terms presented above where chosen. This narrowed the descriptors available to 15. The correlation of these 15 descriptors with $\ln x$ was calculated, and the most correlated ones were retained (where $R^2 > 0.98$), while the remaining descriptors were discarded. This boiled down to only six descriptors. The model was developed using only one descriptor at the time, and afterwards the model was improved by the inclusion of new descriptors. The improved model was tested and if the prediction improved the added descriptor was retained, if not, it was excluded. Models were created by stepwise construction and as a last approach the parent data set was split into two subsets chosen randomly: a training set and an external test set. The training procedure stopped when the error of predictions for the compounds from the internal validation set reached its minimum. Finally, the

Table 2
Correlation parameters derived from the application of Eq. (1) and standard thermodynamic molar properties of solution of ILs in water at 298.15 K (and respective standard deviation, σ).

	$[C_3mpip][Tf_2N]$	$[C_3mpyr][Tf_2N]$	$[C_3mim][Tf_2N]$	$[C_3mpy][Tf_2N]$	$[C_4mpyr][Tf_2N]$
$(A \pm \sigma)$	−127 ± 82	−88 ± 50	−351 ± 20 [11]	−228 ± 77 [9]	−318 ± 189
$(B \pm \sigma)$ (K^{-1})	4604 ± 2990	2990 ± 6174	6365 ± 1011 [11]	9139 ± 3499 [9]	13,266 ± 8509
$(C \pm \sigma)$	18 ± 12	12 ± 20	24 ± 3 [11]	33 ± 12 [9]	46 ± 28
$(\Delta_{sol}H^0_m(T) \pm \sigma)$ (kJ mol^{-1})	7.0 ± 1.5	5.8 ± 1.5	5.9 ± 1.5 [11]	6.5 ± 1.5 [9]	5.2 ± 1.5
$(\Delta_{sol}G^0_m(T) \pm \sigma)$ (kJ mol^{-1})	19.60 ± 0.02	19.18 ± 0.02	18.652 ± 0.001 [11]	19.56 ± 0.02 [9]	20.68 ± 0.01
$(\Delta_{sol}S^0_m(T) \pm \sigma)$ (J K^{-1} mol^{-1})	−42.3 ± 5.1	−44.9 ± 5.1	−42.6 ± 5.0 [11]	−43.9 ± 5.1 [9]	−51.9 ± 5.1

models created were validated with the ILs from the external test set. Models were fitted for ILs-water mutual solubilities at 303.15 K.

3.3. Results and discussion

The target property tested in this work was the liquid saturation behavior between ILs and water, at a fixed temperature, by applying a QSPR approach. QSPR methods are based on the concept that all the information related to a molecule, in this specific case an ion, is set in its chemical structure.

For the cations, the following models were fitted and tested maintaining a common anion ($[Tf_2N]$).

$$\ln x = a + b \times S_p \quad (3)$$

$$\ln x = a + b \times S_v \quad (4)$$

$$\ln x = a + b \times S_p + c \times S_v \quad (5)$$

where S_p is the sum of atomic polarizabilities and S_v is the sum of atomic van der Waals volumes, both scaled on carbon atom and both belonging to the constitutional descriptors.

Once the model was fitted for the cations, a descriptor to take into account the contribution of the anion was introduced into this general model. The choice of this descriptor followed the procedure outlined above for cations. The one chosen was J_{hetp} (Balaban-type index from polarizability weighted distance matrix – topological descriptor) and the final relationship, described in the following Eq. (6), was used in all the further calculations.

$$\ln x = m_0 + m_1 \times S_p(\text{cation}) + m_2 \times S_v(\text{cation}) + m_3 \times J_{hept}(\text{anion}) \quad (6)$$

In general, the mutual solubilities between ILs and water are described as the sum of a cation and an anion contribution, where the anion contribution J_{hept} is maintained as a constant value and independent of the cation family and nature, while the remaining coefficients are further adjusted to the experimental data. This pathway of correlating the experimental data was based on the idea that the IL anion is the main determining factor ruling the ILs-water liquid–liquid equilibria [9]. The final correlation obtained was achieved with four latent variables and three descriptors (two for the IL cation and one for the IL anion).

In order to estimate the parameters in the model described by Eq. (6) the 26 ILs were divided into two sets: 17 for a training set and 9 for a test set, chosen randomly. For the water solubility in the IL-rich phase the optimized adjusted parameters were $m_0 = -0.6041$, $m_1 = -0.2911$, $m_2 = 0.2796$ and $m_3 = -0.0566$, while for the solubil-

Table 3
Descriptors, ln of experimental data and ln of calculated values for the solubility of water in ILs (x_w) and solubility of ILs in water (x_{IL}) at 303.15 K, and relative deviations of calculated values from experimental data (δ).

IL		Descriptors			Experimental ln x_w	Calculated ln x_w	δ (%)	Experimental ln x_{IL}	Calculated ln x_{IL}	δ (%)
Cation	Anion	S_p	S_v	J_{hetp}						
Training set										
$[C_4mim]$	$[PF_6]$	14.96	13.87	2.908	−1.228	−1.245	1.5	−6.656	−6.524	2.0
$[C_6mim]$[9]		18.48	17.07		−1.386	−1.375	0.8	−7.667	−7.619	0.6
$[C_8mim]$[9]		22.01	20.26		−1.528	−1.511	1.1	−8.835	−8.672	1.8
$[C_3mpy]$[20]		14.95	13.88		−1.221	−1.240	1.6	−6.220	−6.565	5.5
$[C_1mim]$[20]	$[Tf_2N]$	9.68	9.08	3.932	−1.017	−1.106	8.7	−6.535	−6.338	3.0
$[C_3mim]$[11]		13.20	12.28		−1.251	−1.236	1.3	−7.473	−7.432	0.5
$[C_4mim]$[11]		14.96	13.87		−1.304	−1.303	0.0	−8.054	−7.957	1.2
$[C_6mim]$[11]		18.48	17.07		−1.520	−1.433	5.7	−9.238	−9.051	2.0
$[C_7mim]$[11]		20.24	18.67		−1.570	−1.498	4.5	−9.849	−9.599	2.5
$[C_{10}mim]$[20]		25.53	23.46		−1.604	−1.699	5.9	–	–	–
$[C_2C_2im]$[20]		13.20	12.28		−1.224	−1.236	1.0	−7.488	−7.432	0.7
$[C_3mpy]$[9]		14.95	13.88		−1.347	−1.298	3.7	−7.850	−7.997	1.9
[4-C_4mpy] [20]		16.72	15.48		−1.325	−1.366	3.1	−8.242	−8.527	3.5
$[C_4py]$[20]		14.95	13.88		−1.311	−1.563	1.1	−9.967	−10.146	2.1
$[C_8py]$[20]		22.00	20.27		−1.535	−1.298	1.9	−7.832	−7.997	1.8
$[C_3mpip]$		17.24	15.67		−1.465	−1.464	0.1	−7.860	−8.038	2.3
$[C_3mpyr]$		15.48	14.08		−1.370	−1.396	1.9	−7.640	−7.514	1.6
Test set										
$[C_3mim]$[20]	$[PF_6]$	13.20	12.28	2.908	−1.149	−1.178	2.5	−5.969	−6.000	0.4
$[C_4C_1mim]$[9]		16.72	15.47		−1.519	−1.310	13.7	−7.042	−7.071	0.4
$[C_2mim]$[11]	$[Tf_2N]$	11.44	10.68	3.932	−1.165	−1.171	0.5	−7.041	−6.885	2.2
$[C_5mim]$[11]		16.72	15.47		−1.459	−1.368	6.2	−8.512	−8.504	0.1
$[C_8mim]$[11]		22.01	20.26		−1.635	−1.569	4.0	−10.246	−10.105	1.4
$[C_4C_1mim]$[20]		16.72	15.47		−1.552	−1.368	11.8	−8.430	−8.504	0.9
$[C_4mpy]$[20]		16.72	15.48		−1.454	−1.366	6.1	−8.336	−8.527	2.3
$[C_6py]$[20]		18.48	17.08		−1.402	−1.431	2.1	−8.242	−9.074	10.1
$[C_4mpyr]$		17.24	15.67		−1.457	−1.464	0.5	−8.373	−8.038	4.0

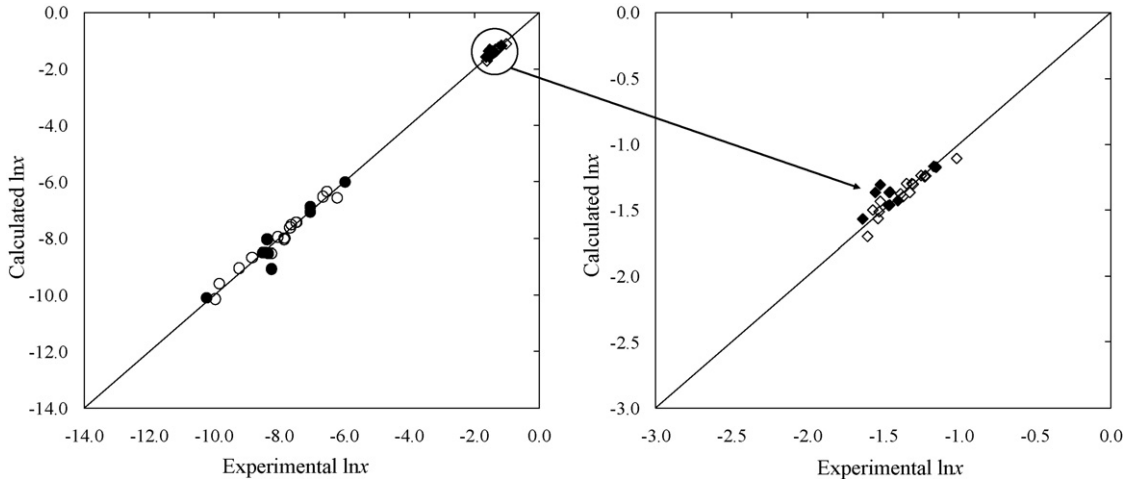

Fig. 3. Calculated $\ln x$ as a function of experimental $\ln x$: (○, ●) Mole fraction solubility of ILs in water; (◊, ♦) Mole fraction solubility of water in ILs (open symbols: training set; full symbols: test set).

ity of ILs in the aqueous-rich phase the parameters obtained were $m_0 = 2.8186$, $m_1 = 1.7800$, $m_2 = -2.3001$ and $m_3 = -1.3992$. Table 3 shows the descriptors calculated, as well as the experimental data and calculated values that result from the application of Eq. (6) for the mutual solubilities between water and ILs at 303.15 K. The respective relative deviations (δ) between the calculated values and the experimental data are also presented in Table 3. In addition, it was performed an ANOVA analysis for both models and the $F_{adjusted}$ showed to be higher than F_{critic}. The values obtained to $F_{adjusted}$ were 39.29 for solubility of water in ILs and 129.3 for the solubility of ILs in water. Comparing to F_{critic} (3.49 for $\ln x_w$ and 3.41 for $\ln x_{IL}$) it can be concluded that both models fit well to the experimental values. In Fig. 3 it is shown the plot of calculated *vs*. experimental data for all the ILs studied in this work.

The proposed model shows average deviations for the calculated values of the water solubility in ILs and ILs solubility in water of 4% and 2%, respectively. Nevertheless, higher deviations for the trisubstituted ILs are observed for the water solubility in ILs, compared to the monosubstituted and disubstituted ILs. However, for the solubility of the trisubstituted ILs in water the deviations are low. From the analysis of Table 3, it is possible to see that the calculated value for both phases for $[C_4C_1mim][Tf_2N]$ is equal to $[C_5mim][Tf_2N]$. Indeed, it was shown before [9] that the behavior of $[C_4C_1mim][PF_6]$ is different for the aqueous-rich and IL-rich phases. This model predicted the same behavior for both phases which resulted in a higher deviation for solubility of water in cations with three alkyl substitutions. The presence of three alkyl substituents at the cation, with the elimination of the most acidic hydrogen at the position C2, is one of the major shortcomings of the QSPR model proposed that could result from an overestimation of the hydrogen bonding interactions between ILs and water since there is not enough experimental data for trisubstituted IL cations.

4. Conclusions

A new pathway for the quantification of ILs solubility in water using ESI-MS was here demonstrated, and original data for pyrrolidinium- and piperidinium-based ILs, in the temperature range between (288.15 and 318.15) K, were presented. The ILs solubility in water decreases with the alkyl side chain length increase at the cation and from piperidinium- to pyridinium- to pyrrolidinium- to imidazolium-based ILs. Contrary to what was observed before for the IL-rich phase [9] where the solubility of water in ILs largely depends on the IL availability of electrons for privileged interactions, the solubility of ILs in water is primarily defined by the cation size, and to a lower extent, on their aromaticity. The standard molar thermodynamic functions of solution, derived from experimental solubility data, indicate that the ILs dissolution in water is an endothermic and entropic driven process.

The QSPR approach here developed is a valuable tool to predict mutual solubilities between water and ILs. Good correlations were obtained with the training set and reasonable predictions obtained within the test set of ILs. With the exception for the water solubility in $[C_4C_1mim]$-based ILs, the deviations of the model are smaller than 10%. The QSPR model presented in this work could thus help in the molecular design of ILs for specific applications.

Acknowledgments

The authors thank financial support from Fundação para a Ciência e a Tecnologia: project PTDC/EQU-FTT/65252/2006 and PhD grants SFRH/BD/28258/2006 and SFRH/BD/37830/2007 from M.J.P. and S.P.M.V., respectively.

Appendix A. Supplementary data

Supplementary data associated with this article can be found, in the online version, at doi:10.1016/j.fluid.2009.12.035.

References

[1] K.N. Marsh, J.A. Boxall, R. Lichtenthaler, Fluid Phase Equilib. 219 (2004) 93–98.
[2] S. Pandey, Anal. Chim. Acta 556 (2006) 38–45.
[3] T. Welton, Coord. Chem. Rev. 248 (2004) 2459–2477.
[4] M.J. Earle, J.M.S.S. Esperança, M.A. Gilea, J.N. Canongia Lopes, L.P.N. Rebelo, J.W. Magee, K.R. Seddon, J.A. Widegren, Nature 439 (2006) 831–834.
[5] D. Zhao, Y. Liao, Z. Zhang, Clean 35 (2007) 42–48.
[6] J. Ranke, A. Müller, U. Bottin-Weber, F. Stock, S. Stolte, J. Arning, R. Störmann, B. Jastorff, Ecotoxicol. Environ. Saf. 67 (2007) 430–438.
[7] J. Ranke, A. Othamn, P. Fan, A. Müller, Int. J. Mol. Sci. 10 (2009) 1271–1289.
[8] D.J. Couling, R.J. Bernot, K.M. Docherty, J.K. Dixon, E.J. Maggin, Green Chem. 8 (2006) 82–90.
[9] M.G. Freire, C.M.S.S. Neves, P.J. Carvalho, R.L. Gardas, A.M. Fernandes, I.M. Marrucho, L.M.N.B.F. Santos, J.A.P. Coutinho, J. Phys. Chem. B 111 (2007) 13082–13089.
[10] M.G. Freire, L.M.N.B.F. Santos, A.M. Fernandes, J.A.P. Coutinho, I.M. Marrucho, Fluid Phase Equilib. 261 (2007) 449–454.
[11] M.G. Freire, P.J. Carvalho, R.L. Gardas, I.M. Marrucho, L.M.N.B.F. Santos, J.A.P. Coutinho, J. Phys. Chem. B 112 (2008) 1604–1610.
[12] S.P.M. Ventura, A.M.M. Gonçalves, F. Gonçalves, J.A.P. Coutinho, Toxicity evaluation of water immiscible ionic liquids to standard aquatic species, Presented at BATIL – 2 (Biodegrability and Toxicity of Ionic Liquids), Berlin, Germany, 2009.
[13] H. Zhao, S.Q. Xia, P.S. Ma, J. Chem. Technol. Biotechnol. 80 (2005) 1089–1096.
[14] M.L. Dietz, Sep. Sci. Technol. 41 (2006) 2047–2063.
[15] D.C. Stepinski, B.A. Young, M.P. Jensen, P.G. Rickert, J.A. Dzielawa, A.A. Dilger, D.J. Rausch, M.L. Dietz, J. Electrochem. Soc. 933 (2006) 233–247.

[16] P.R.V. Rao, K.A. Venkatesan, T.G. Srinivasan, Prog. Nucl. Energy 50 (2008) 449–453.
[17] Y. Zuo, Y. Liu, J. Chen, D.Q. Li, Ind. Eng. Chem. Res. 47 (2008) 2349–2355.
[18] J. Langmaier, Z. Samec, Electrochem. Commun. 9 (2007) 2633–2638.
[19] M.G. Freire, P.J. Carvalho, R.L. Gardas, L.M.N.B.F. Santos, I.M. Marrucho, J.A.P. Coutinho, J. Chem. Eng. Data 53 (2008) 2378–2382.
[20] C.M.S.S. Neves, M.G. Freire, I.M. Marrucho, L.M.N.B.F. Santos, J.A.P. Coutinho, unpublished data.
[21] J.L. Anthony, E.J. Maginn, J.F. Brennecke, J. Phys. Chem. B 105 (2001) 10942–10949.
[22] D.S.H. Wong, J.P. Chen, J.M. Chang, C.H. Chou, Fluid Phase Equilib. 194–197 (2002) 1089–1095.
[23] J.M. Crosthwaite, S.N.V.K. Aki, E.J. Maginn, J.F. Brennecke, J. Phys. Chem. B 108 (2004) 5113–5119.
[24] L.P.N. Rebelo, V. Najdanovic-Visak, Z.P. Visak, M.N. Ponte, J. Szydlowski, C.A. Cerdeirina, J. Troncoso, L. Romani, J.M.S.S. Esperança, H.J.R. Guedes, H.C. Sousa, Green Chem. 6 (2004) 369–381.
[25] V. Najdanovic-Visak, J.M.S.S. Esperança, L.P.N. Rebelo, M.N. Ponte, H.J.R. Guedes, K.R. Seddon, J. Szydlowski, Phys. Chem. Chem. Phys. 4 (2002) 1701–1703.
[26] U. Domańska, A. Marciniak, Green Chem. 9 (2007) 262–266.
[27] U. Domańska, I. Bakala, J. Pernak, J. Chem. Eng. Data 52 (2007) 309–314.
[28] N. Papaiconomou, N. Yakelis, J. Salminen, R. Bergman, J.M. Prausnitz, J. Chem. Eng. Data 51 (2006) 1389–1393.
[29] N. Papaiconomou, J. Salminen, J.M. Lee, J.M. Prausnitz, J. Chem. Eng. Data 52 (2007) 833–840.
[30] Z.B. Alfassi, R.E. Huie, B.L. Milman, P. Neta, Anal. Bioanal. Chem. 377 (2003) 159–164.
[31] N.V. Shvedene, S.V. Borovskaya, V.V. Sviridov, E.R. Ismailova, I.V. Pletnev, Anal. Bioanal. Chem. 381 (2005) 427–430.
[32] S.J. Gaskell, J. Mass Spectrom. 32 (1997) 677–688.
[33] P. Kebarle, U.H. Verkerk, Mass Spectrom. Rev. 28 (2009) 898–917.
[34] A. Crum-Brown, T.R. Fraser, Trans. R. Soc. Edinburgh 25 (1868–1869) 151–203.
[35] M. Grover, B. Singh, M. Bakshi, S. Singh, Pharma. Sci. Technol. Today 3 (2000) 28–35.
[36] A. Varnek, N. Kireeva, I.V. Tetko, I.I. Baskin, V.P. Solovev, J. Chem. Inf. Mod. 47 (2007) 1111–1122.
[37] R. Bini, M. Malvaldi, W.R. Pitner, C. Chiappe, J. Phys. Org. Chem. 21 (2008) 622–629.
[38] A.M. Fernandes, J.A.P. Coutinho, I.M. Marrucho, J. Mass Spectrom. 44 (2009) 144–150.
[39] R.L. Gardas, H.F. Costa, M.G. Freire, P.J. Carvalho, I.M. Marrucho, I.M.A. Fonseca, A.G.M. Ferreira, J.A.P. Coutinho, J. Chem. Eng. Data 53 (2008) 805–811.
[40] A. Ben-Naim, J. Solution Chem. 30 (2001) 475–487.